Radiotherapy and Oncology 86 (2008) 165—170
www.thegreenjournal.com

Review

Secondary neutrons in clinical proton radiotherapy: A charged issue

David J. Brenner*, Eric J. Hall

Center for Radiological Research, Columbia University Medical Center, NY, USA

Abstract

Hospital-based proton facilities may represent a major advance in radiation therapy, in part because of excellent dose distributions around the tumor, and in part because of the potentially lower whole-body dose compared with photon radiotherapy. Most current proton beams are spread out to cover the tumor using beam scattering and collimation techniques (passive scattering); this will necessarily result in an extra whole-body neutron dose, due to interactions of the protons with the scattering and collimating beam elements. However, the clinical significance of this whole-body low-dose neutron exposure has remained controversial. The number of proton facilities worldwide is increasing rapidly, and most of these facilities are/will be based on passive scattering. Thus it is important to assess and, ideally, minimize, the potential for second cancer induction by secondary neutrons. We discuss here the neutron doses involved, and the associated potential second cancer risks, with an emphasis on the uncertainties involved.

Keywords: Proton radiotherapy; Secondary neutrons; Second cancers; Passive scattering

The development of hospital-based proton facilities represents a major step forward in radiotherapy, in part because of excellent dose distributions around the tumor [1], and in part because of the potentially lower whole-body dose compared with photon radiotherapy [2]. In the context of the whole-body dose, however, the issue of secondary neutrons produced by the scattering components of passively scattered radiotherapeutic proton beams has recently attracted much research and considerable discussion [3—20]. Whilst there has been a justifiable focus on establishing the neutron doses involved [7—20], there is still no agreement about whether these scattered neutrons really represent a clinically relevant issue.

To briefly summarize the issue: for most practical proton radiotherapy, it is necessary to spread out the narrow pencil beam produced by a proton accelerator, in order to provide uniform coverage over the target. This can be done, as in most current proton radiotherapy facilities, by inserting scattering material into the beam (passive scattering [9,21]), or by using deflecting magnets to sweep the beam across the tumor (active scanning [22,23]). Because passive scattering necessarily introduces a number of material components into the beamline, proton interactions with these components result in the production of high-energy secondary neutrons not present in actively scanned proton beams. In clinical proton beams, the largest source of these neutrons is generally the final collimator, located close to the patient; this collimator is fabricated out of brass with a patient-specific aperture shaped to match the target. The proton beam is always larger than this aperture, to a lesser or greater extent, so protons will bombard the brass collimator and produce secondary neutrons.

The number of proton facilities worldwide is increasing rapidly [24], and most of these facilities are/will be based on passive scattering. In this light, and in light of the significant carcinogenicity of low-dose neutron exposures [25], it is important to assess and, ideally, minimize, the potential for second cancer induction by these secondary neutrons.

Measurements and calculations of neutron doses in clinical proton beams

Measured neutron doses from clinical proton facilities vary greatly [8,11,14—19], partly as a result of different measurement techniques, and partly as a result of different beam geometries. It is notoriously hard to measure high-energy neutron doses in a mixed radiation field, and it is still harder to make neutron measurements in realistic anthropomorphic phantom — which is what is needed to estimate organ doses and thus risks. A practical alternative for neutron dose estimation is to use a Monte-Carlo approach in which the entire treatment setup, as well as an anthropomorphic phantom, is simulated. This general approach has been well validated [26], and has been used by Paganetti

0167-8140/$ - see front matter doi:10.1016/j.radonc.2007.12.003

Table 1
Calculated neutron doses to selected radiogenic organs for a three-field proton therapy plan at the passively modulated NPTC facility, treating a lung tumor with a planned 72 Gy GTV dose

Organ	Neutron dose (mGy)	
	Internal	External
Red bone marrow	28	16
Colon	0	4
Lung (out-of-field)	39	34
Stomach	0	20
Bladder	0	3
Breast	1	24
Liver	1	32
Esophagus	2	29
Thyroid	1	32
Brain	0	12
Kidney	0	19
Pancreas	0	22

Data derived from Jiang et al. [10]. ''Internal'' refers to neutrons produced by proton interactions in the body. ''External'' refers to neutrons produced by proton interactions in the scattering elements of the passively modulated beamline.

and colleagues [10], and others [7], to calculate out-of-field organ-specific neutron doses in clinical proton beams. The same approach has also been used to quantitate out-of-field neutron doses in high-energy photon fields [27] and in boron neutron capture therapy [28].

In particular, Paganetti and colleagues [10] used the Geant-4 radiation transport toolkit [26] to simulate the relevant parts of the proton beam line at the Northeast Proton Therapy Center (NPTC) at Mass General Hospital [29], together with a realistic voxel based whole-body patient model (VIP Man [30]). Table 1 shows calculated neutron-induced organ doses, derived from Ref. [10], for a three-field proton therapy plan at the NPTC, for a lung tumor with a planned GTV dose of 72 Gy. The neutron doses are divided into the internal neutron dose, resulting from proton interactions in the body (which is essentially irreducible), and the external neutron dose, resulting from proton interactions with the elements of the NPTC passive focusing system (which is largely avoidable by using an active proton scanning system [15]).

The neutron doses in Table 1 are sufficiently small that they will not cause classic early or late radiation sequelae. However, low neutron doses have been well established to have a high potential for carcinogenesis [25]; so, particularly as one of the putative advantages of protons relates to a potential reduction in second cancer risks, it is important to quantitate the neutron-related second cancer risk.

Second cancer risk estimation from secondary neutrons

High-energy neutron RBEs at low doses

To estimate a cancer risk from these neutrons, an RBE (relative biological effect) factor must be applied to standard low-LET cancer risk estimates. In general this RBE is dose dependent, but at low doses the RBE tends to a constant value, usually called the maximal RBE (RBE_M [25]). In general neutron RBEs for relevant endpoints (carcinogenesis or life shortening) are uncertain because there is limited human experience to draw upon, and also because there is a comparatively small relevant database in animals or using *in-vitro* models of carcinogenesis. The most pertinent quantitative data for low-dose neutron carcinogenesis are summarized in Fig. 1 for humans, and in Table 2 for mice. Based on the human experience (see Fig. 1), using what are now considered to be realistic neutron dose estimates to A-bomb survivors [31,32], two independent groups have estimated the most likely RBE_M for neutron-induced carcinogenesis in humans, respectively, as 100 [95% CI: 25—400] for solid-cancer mortality [33], and as 63 [95% CI: 0—275] for overall cancer incidence [34]. The results of the most comprehensive quantitative neutron carcinogenesis studies in animals [25,35—37] are summarized in Table 2. As might be expected, there is considerable variation in different tissues, but a crude average of the results gives an RBE_M estimate of 30 ± 17.

A second major issue in estimating a neutron RBE in the proton radiotherapy context is the neutron energy dependence. Specifically, essentially all the available human and animal data for neutron carcinogenesis come from fission neutrons, where almost all of the dose is delivered by neutrons of energies <10 MeV. By contrast, neutrons produced in a proton-therapy context are themselves of high energy, with less than 3% of the neutron dose resulting from interac-

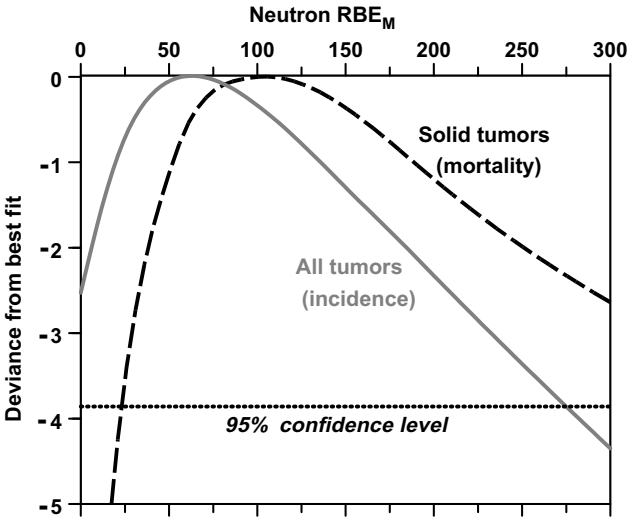

Fig. 1. The curves represent the quality of fit of standard risk models to cancer incidence and mortality data in A-bomb survivors, who were exposed to a mixed photon/neutron field [31,32], as a function of assumed values of the neutron RBE_M. The zero values represent the neutron RBEs which give the best fit to the A-bomb data, and the neutron RBEs where the curves intersect the dotted line represent the 95% confidence limits surrounding the best fit. Thus, for solid tumor mortality (dashed curve), the best fit to the A-bomb data involves an estimated RBE_M of 100 [95% CI: 25—400] [33], and for cancer incidence (solid curve), the best fit to the A-bomb data involves an estimated RBE_M of 63 [95% CI: 0—275] [34].

Table 2
Estimated low-dose RBE values for fission neutron-induced carcinogenesis in mice

Mouse strain/endpoint	Measured RBE_M
RFM/thymic lymphoma	27 ± 26
RFM/pituitary	59 ± 52
RFM/Harderian gland	36 ± 10
RFM/lung tumor	6 ± 3
BALB/c lung adenocarcinoma	19 ± 6
BALB/c mammary carcinoma	33 ± 12
Overall	30 ± 17

Data from Refs. [35–37], and analysis from Ref. [25].

tions by neutrons with energy less than 10 MeV and more than about 2/3 of the dose comes from neutrons with energies over 100 MeV ([20], and see Fig. 2). Thus a technique is needed to extrapolate the energy dependence of the measured neutron RBE_M to much higher neutron energies. In the absence of relevant high-energy neutron carcinogenesis data, this has typically been done [25,38–41] using radiation weighting factors based on extensive measurements of dicentric chromosome aberration induction in human lymphocytes, as a function of neutron energy [42,43]. However the available chromosome aberration data used in those analyses extended to a maximum neutron energy of 14 MeV which, as we have seen, is much lower than the neutron energy range of interest here.

In fact, since the most recent of the chromosome-aberration based neutron-energy analyses was completed by the ICRP in 1990 ([39], more recent ICRP reanalyses [40] have focused only on lower energies), an RBE_M measurement for dicentric chromosome aberrations in human lymphocytes has been reported from CERN in Geneva [44], for a high-energy neutron spectrum [45] which is qualitatively similar to those of interest here [20]. The neutron spectrum used in that CERN study is compared in Fig. 2 to the calculated neutron spectrum downstream of a passive scanning proton nozzle, at the MD Anderson proton facility [20]. The measured [44] RBE_M for this CERN neutron spectrum (based on a fractionated neutron dose of 2.5 mGy) was 96 (CI: 67–148). By contrast, the predicted RBE_M for this CERN neutron spectrum, based on the ICRP/NCRP extrapolations to high neutron doses, is 8.

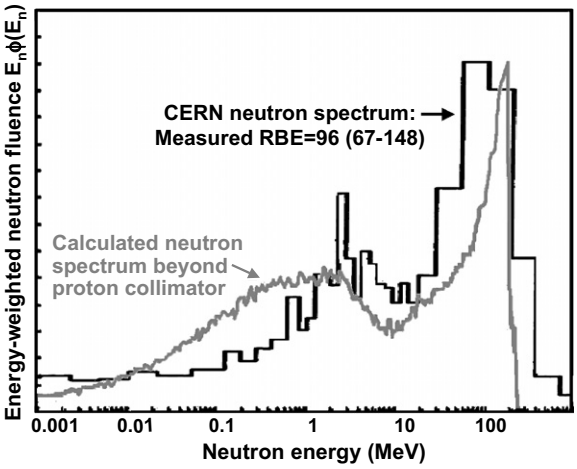

Fig. 2. Comparison of energy spectrum of CERN neutron field [45] used in neutron RBE measurements by Heimers [44], compared with the estimated neutron spectrum [20] directly downstream of the final patient collimator at the MD Anderson clinical proton facility.

While the CERN experiment is suggestive of a high RBE for high-energy neutrons, it is important to stress that it represents only a single report. It should also be emphasized that the endpoint of dicentric chromosome aberrations in peripheral blood lymphocytes, used there and in all the ICRP/ICRU/NCRP extrapolations of neutron RBE to high doses, may well be a poor surrogate for radiation-induced cancer; while exchange-type chromosome aberrations are linked to leukemias, they are comparatively rarely associated with solid cancers [46].

In principle, we should also consider the effects of fractionation on the RBE, and a formalism for doing this is available [47–49]. However, at low doses, the effect of fractionation on RBE is expected to be small [49].

We can conclude that there are major uncertainties associated with the low-dose RBE of the very high-energy neutrons associated with proton radiotherapy, the limited available evidence suggesting that the NCRP/ICRP high-energy neutron radiation weighting factors may underestimate these high-energy neutron RBEs. Based on these considerations, a conservative estimate of the RBE_M for neutron carcinogenesis would be 25. It is certainly possible that an RBE_M value of 25 is an overestimate, but the weight of evidence, but based on the human and animal data for fission neutrons, and the chromosome aberration data for a neutron spectrum similar to the ones of interest here, an RBE_M estimate of 25 for neutron carcinogenesis is probably a conservative estimate. Hereafter, we shall use this value of 25, but it is important to bear in mind that it is associated with uncertainty of about a factor of 4 in each direction.

Estimated second cancer risks from secondary neutrons in proton radiotherapy

Table 3 shows the estimated neutron equivalent doses to relevant organs, based on the neutron dose estimates in Table 1 and an RBE_M estimate of 25. These organ-specific equivalent doses can then be utilized to calculate lifetime cancer risks, using standard techniques such as those described in the US National Academy of Sciences BEIR-VII report [50] and other radiation risk estimation reports. Specifically, age-, gender- and organ-specific cancer risks from A-bomb survivors are transferred to lifetime cancer risks in a Western population using techniques described, for example, by Land et al. [51]. Shown in Table 3 are estimated organ-specific and summed lifetime second cancer risks induced by external neutrons for a 15 year male and female, assuming that the patient is cured of his/her primary cancer. The overall lifetime cancer risk estimates for a 15 year old (in the case considered here, ~5% for a male, ~10% for a female) would, of course, be larger for a still younger patient, and smaller for an older patient. We emphasize the risks for a young patient, in that one of the

Table 3
Columns 2 and 3: Estimated neutron doses from Table 1 (for a proton therapy lung-tumor plan at the passively modulated NPTC facility), weighted with an estimated RBE_M value of 25

Organ	Neutron equivalent dose (mSv)		Lifetime cancer risk (%) due to external neutrons in a cured 15 year old[a]	
	Internal	External	Male	Female
Red bone marrow	702	397	0.42	0.30
Colon	1	88	0.18	0.12
Lung (out-of-field)	968	851	1.53	3.55
Stomach	12	508	0.23	0.31
Bladder	1	70	0.09	0.09
Breast	33	596	—	3.30[b]
Liver	36	802	0.29	0.13
Esophagus	59	734	0.51	0.28
Thyroid	32	788	0.26	1.40
Brain	4	288	0.05	0.10
Kidney	6	471	0.90	1.14
Pancreas	10	559	0.21	0.41
Total			4.7	11.1

Columns 4 and 5: Corresponding estimated lifetime organ-specific second cancer risks due to externally produced neutrons, for a patient aged 15, assuming the patient is cured of his/her primary tumor. Summary data for other ages at exposure are shown in Fig. 3.
[a] Lifetime risk estimates for leukemia, colon, lung, stomach, bladder, breast, liver, and thyroid based on data in the recent BEIR-VII report [47]. Lifetime risks for esophagus, brain, kidney and pancreas based on data from the IREP software developed by Land and colleagues [48].
[b] Based on breast dose calculated for male phantom.

prima-facie advantages of proton therapy is to minimize the second cancer risk for young patients with a potentially long life expectancy, but Fig. 3 also shows the estimated summed cancer risks, calculated as in Table 3, for older patients.

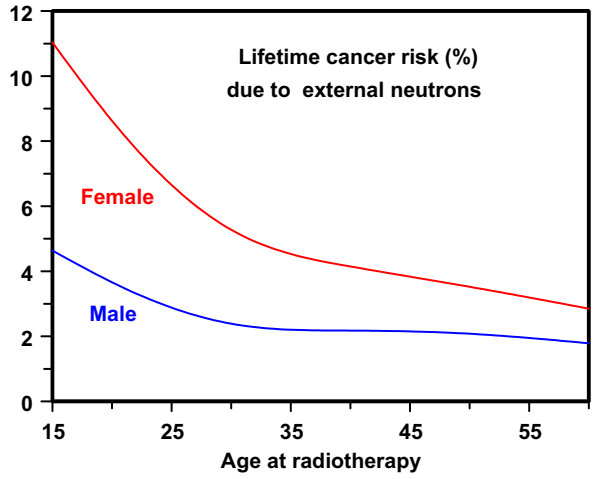

Fig. 3. Total estimated lifetime second cancer risks due to externally produced neutrons, for a 72 Gy proton therapy lung-tumor plan at the passively modulated NPTC facility, assuming the patient is cured of his/her primary tumor. Organ-specific risks are estimated, as in Table 3, from the organ-specific equivalent doses shown in Table 3, and then summed. It is important to emphasize the uncertainties associated with these risk estimates, as discussed in the text.

Conclusions

Of course some radiation-induced second cancer risk is an unavoidable consequence of any radiotherapeutic protocol, and the neutron-induced second cancer risks estimated here are not dissimilar from the second cancer risks inherent in photon-based intensity-modulated radiation therapy [52,53]. A difference is that the second cancer risks from externally generated neutrons in a passively scanned proton beam are (a) more uncertain, (b) reducible through optimized beamline design, and (c) avoidable through the use of an active scanning system.

Regarding the issue of actively- *vs.* passively scanned proton beams, it is pertinent to note that the technology required for actively scanned proton beams, which would avoid this external neutron problem, is relatively complex, requiring high instantaneous dose rates and sophisticated control systems; in particular there may be a greater potential for dose delivery errors due to patient motion [23,54–56]. Nevertheless, one active-scanning system is in clinical use [57–59], and plans are ongoing for their introduction into many of the major proton radiotherapy facilities that currently use passive scanning [60–62].

In the meantime, it would be highly desirable to optimize the geometry of the current generation of passively modulated proton beamlines, in order to reduce the neutron dose to the patient. Two complementary approaches are possible: the first is to better match the beam broadening devices with the beam size being used, which would reduce the number of protons incident on the final patient collimator; this is really a practical matter of how easily different beamline ''snouts'' can be interchanged. The other comple-

mentary approach, given that a patient collimator will always be needed in a passively scanned proton beamline, is to optimize the collimator design. In particular, most proton collimators are currently made out of brass or cerrobend, which are high atomic-mass materials; because neutron production increases with increasing atomic mass [63,64], a collimator made out of lower-mass high-density material could significantly decrease the neutron dose and thus the neutron-related second cancer risk.

* **Corresponding author. David J. Brenner**, Center for Radiological Research, Columbia University Medical Center, 630 West 168th Street, New York, NY 10032, USA. *E-mail address:* djb3@columbia.edu

Received 19 September 2007; received in revised form 7 December 2007; accepted 7 December 2007; Available online 14 January 2008

References

[1] Chang JY, Zhang X, Wang X, et al. Significant reduction of normal tissue dose by proton radiotherapy compared with three-dimensional conformal or intensity-modulated radiation therapy in Stage I or Stage III non-small-cell lung cancer. Int J Radiat Oncol Biol Phys 2006;65:1087–96.

[2] Miralbell R, Lomax A, Cella L, Schneider U. Potential reduction of the incidence of radiation-induced second cancers by using proton beams in the treatment of pediatric tumors. Int J Radiat Oncol Biol Phys 2002;54:824–9.

[3] Hall EJ. Intensity-modulated radiation therapy, protons, and the risk of second cancers. Int J Radiat Oncol Biol Phys 2006;65:1–7.

[4] Gottschalk B. Neutron dose in scattered and scanned proton beams: in regard to Hall EJ (Int J Radiat Oncol Biol Phys 2006;65:1–7). Int J Radiat Oncol Biol Phys 2006;66:1594; author reply 1595.

[5] Macklis R. In regard to Hall: intensity-modulated radiation therapy, protons, and the risk of second cancers (Int J Radiat Oncol Biol Phys 2006;65:1–7). Int J Radiat Oncol Biol Phys 2006;66:1593–4; author reply 1595.

[6] Paganetti H, Bortfeld T, Delaney TF. Neutron dose in proton radiation therapy: in regard to Hall EJ (Int J Radiat Oncol Biol Phys 2006;65:1–7). Int J Radiat Oncol Biol Phys 2006;66:1594–5; author reply 1595.

[7] Agosteo S, Birattari C, Caravaggio M, Silari M, Tosi G. Secondary neutron and photon dose in proton therapy. Radiother Oncol 1998;48:293–305.

[8] Binns PJ, Hough JH. Secondary dose exposures during 200 MeV proton therapy. Radiat Prot Dosimetry 1997;70:441–4.

[9] Fontenot JD, Newhauser WD, Titt U. Design tools for proton therapy nozzles based on the double-scattering foil technique. Radiat Prot Dosimetry 2005;116:211–5.

[10] Jiang H, Wang B, Xu XG, Suit HD, Paganetti H. Simulation of organ-specific patient effective dose due to secondary neutrons in proton radiation treatment. Phys Med Biol 2005;50:4337–53.

[11] Mesoloras G, Sandison GA, Stewart RD, Farr JB, Hsi WC. Neutron scattered dose equivalent to a fetus from proton radiotherapy to the mother. Med Phys 2006;33:2479–90.

[12] Polf JC, Newhauser WD. Calculations of neutron dose equivalent exposures from range-modulated proton therapy beams. Phys Med Biol 2005;50:3859–73.

[13] Polf JC, Newhauser WD, Titt U. Patient neutron dose equivalent exposures outside of the proton therapy treatment field. Radiat Prot Dosimetry 2005;115:154–8.

[14] Roy SC, Sandison GA. Scattered neutron dose equivalent to a fetus from proton therapy of the mother. Radiat Phys Chem 2004;71:997–8.

[15] Schneider U, Agosteo S, Pedroni E, Besserer J. Secondary neutron dose during proton therapy using spot scanning. Int J Radiat Oncol Biol Phys 2002;53:244–51.

[16] Schneider U, Fiechtner A, Besserer J, Lomax A. Neutron dose from prostheses material during radiotherapy with protons and photons. Phys Med Biol 2004;49:N119–24.

[17] Tayama R, Fujita Y, Tadokoro M, Fujimaki H, Sakae T, Terunuma T. Measurement of neutron dose distribution for a passive scattering nozzle at the Proton Medical Research Center (PMRC). Nucl Instrum Methods Phys Res A 2006;564:532–6.

[18] Wroe A, Rosenfeld A, Schulte R. Out-of-field dose equivalents delivered by proton therapy of prostate cancer. Med Phys 2007;34:3449–56.

[19] Yan X, Titt U, Koehler AM, Newhauser WD. Measurement of neutron dose equivalent to proton therapy patients outside of the proton radiation field. Nucl Instrum Methods Phys Res A 2002;476:429–34.

[20] Zheng Y, Newhauser W, Fontenot J, Taddei P, Mohan R. Monte Carlo study of neutron dose equivalent during passive scattering proton therapy. Phys Med Biol 2007;52:4481–96.

[21] Koehler AM, Schneider RJ, Sisterson JM. Flattening of proton dose distributions for large-field radiotherapy. Med Phys 1977;4:297–301.

[22] Lomax AJ, Bohringer T, Bolsi A, et al. Treatment planning and verification of proton therapy using spot scanning: initial experiences. Med Phys 2004;31:3150–7.

[23] Jones DTL, Schreuder AN. Magnetically scanned proton therapy beams: rationales and principles. Radiat Phys Chem 2001;61:615–8.

[24] Olsen DR, Bruland OS, Frykholm G, Norderhaug IN. Proton therapy – a systematic review of clinical effectiveness. Radiother Oncol 2007;83:123–32.

[25] NCRP. National council on radiation protection and measurements. The relative biological effectiveness of radiations of different quality. NCRP Report 104; 1990.

[26] Rodrigues P, Trindade A, Peralta L, Alves C, Chaves A, Lopes MC. Application of GEANT4 radiation transport toolkit to dose calculations in anthropomorphic phantoms. Appl Radiat Isot 2004;61:1451–61.

[27] Barquero R, Edwards TM, Iniguez MP, Vega-Carrillo HR. Monte Carlo simulation estimates of neutron doses to critical organs of a patient undergoing 18 MV X-ray LINAC-based radiotherapy. Med Phys 2005;32:3579–88.

[28] Ferrari P, Gualdrini G, Nava E, Burn KW. Preliminary evaluations of the undesirable patient dose from a BNCT treatment at the ENEA-TAPIRO reactor. Radiat Prot Dosimetry, in press.

[29] Paganetti H, Jiang H, Lee SY, Kooy HM. Accurate Monte Carlo simulations for nozzle design, commissioning and quality assurance for a proton radiation therapy facility. Med Phys 2004;31:2107–18.

[30] Xu XG, Chao TC, Bozkurt A. VIP-Man: an image-based whole-body adult male model constructed from color photographs of the Visible Human Project for multi-particle Monte Carlo calculations. Health Phys 2000;78:476–86.

[31] Egbert SD, Kerr GD, Cullings HM. DS02 fluence spectra for neutrons and gamma rays at Hiroshima and Nagasaki with fluence-to-kerma coefficients and transmission factors for sample measurements. Radiat Environ Biophys 2007;46:311–25.

[32] Nolte E, Ruhm W, Loosli HH, et al. Measurements of fast neutrons in Hiroshima by use of Ar-39. Radiat Environ Biophys 2006;44:261–71.

[33] Kellerer AM, Ruhm W, Walsh L. Indications of the neutron effect contribution in the solid cancer data of the A-bomb survivors. Health Phys 2006;90:554–64.

[34] Little MP. Estimates of neutron relative biological effectiveness derived from the Japanese atomic bomb survivors. Int J Radiat Biol 1997;72:715–26.
[35] Ullrich RL. Tumor induction in BALB/c female mice after fission neutron or gamma irradiation. Radiat Res 1983;93:506–15.
[36] Ullrich RL. Tumor induction in BALB/c mice after fractionated or protracted exposures to fission-spectrum neutrons. Radiat Res 1984;97:587–97.
[37] Ullrich RL, Jernigan MC, Cosgrove GE, Satterfield LC, Bowles ND, Storer JB. The influence of dose and dose rate on the incidence of neoplastic disease in RFM mice after neutron irradiation. Radiat Res 1976;68:115–31.
[38] ICRU. The quality factor in radiation protection. Bethesda, MD, Report 40: International Commission on Radiation Units and Measurements.
[39] ICRP. 1990 Recommendations of the International Commission on Radiological Protection: Report 60. Oxford: Pergamon Press; 1991.
[40] ICRP. Relative biological effectiveness (RBE), quality factor (Q), and radiation weighting factor (w_R). Report 92 of the International Commission on Radiological Protection. Ann ICRP 2003;33:1–117.
[41] NCRP. National council on radiation protection and measurements. Calibration of survey instruments used in radiation protection for the assessment of ionizing radiation fields and radioactive surface contamination. NCRP Report 112. Bethesda, MD; 1991.
[42] Lloyd DC, Purrott RJ, Dolphin GW, Edwards AA. Chromosome aberrations induced in human lymphocytes by neutron irradiation. Int J Radiat Biol Relat Stud Phys Chem Med 1976;29:169–82.
[43] Sevan'kaev AV, Zherbin EA, Obaturov GM, Kozlov VM, Tiatte EG. Cytogenetic effects induced in vitro in human peripheral blood lymphocytes by neutrons. II. Relative biological effectiveness of neutrons having different energies. Genetika 1979;15:1228–34 [in Russian].
[44] Heimers A. Cytogenetic analysis in human lymphocytes after exposure to simulated cosmic radiation which reflects the inflight radiation environment. Int J Radiat Biol 1999;75:691–8.
[45] Mitaroff A, Silari M. The CERN-EU high-energy reference field (CERF) facility for dosimetry at commercial flight altitudes and in space. Radiat Protect Dosim 2002;102:7–22.
[46] Mitelman F, Johansson B, Mertens FE. Mitelman Database of chromosome aberrations in cancer. http://cgap.nci.nih.gov/Chromosomes/Mitelman. 2007.
[47] Kellerer A, Rossi H. A generalized formulation of dual radiation action. Radiat Res 1978;75:471–88.
[48] Joiner MC, Field SB. The response of mouse skin to irradiation with neutrons from the 62 MV cyclotron at Clatterbridge, U.K.. Radiother Oncol 1988;12:153–66.
[49] Dale RG, Jones B. The assessment of RBE effects using the concept of biologically effective dose. Int J Radiat Oncol Biol Phys 1999;43:639–45.
[50] National Research Council of the National Academies. Health risks from exposure to low levels of ionizing radiation – BEIR VII. Washington, DC: The National Academies Press; 2006.
[51] Land CE, Gilbert E, Smith JM. Report of the NCI-CDC working group to revise the 1985 NIH radioepidemiological tables. NIH Publication 03-5387. See also www.irep.nci.nih.gov. Bethesda: NIH; 2003. Report No.: NIH 03-5387.
[52] Kry SF, Salehpour M, Followill DS, et al. The calculated risk of fatal secondary malignancies from intensity-modulated radiation therapy. Int J Radiat Oncol Biol Phys 2005;62:1195–203.
[53] Hall EJ, Wuu CS. Radiation-induced second cancers: the impact of 3D-CRT and IMRT. Int J Radiat Oncol Biol Phys 2003;56:83–8.
[54] Phillips MH, Pedroni E, Blattmann H, Boehringer T, Coray A, Scheib S. Effects of respiratory motion on dose uniformity with a charged particle scanning method. Phys Med Biol 1992;37:223–34.
[55] Lambert J, Suchowerska N, McKenzie DR, Jackson M. Intrafractional motion during proton beam scanning. Phys Med Biol 2005;50:4853–62.
[56] Grozinger SO, Rietzel E, Li Q, Bert C, Haberer T, Kraft G. Simulations to design an online motion compensation system for scanned particle beams. Phys Med Biol 2006;51:3517–31.
[57] Timmermann B, Schuck A, Niggli F, et al. Spot-scanning proton therapy for malignant soft tissue tumors in childhood: first experiences at the Paul Scherrer Institute. Int J Radiat Oncol Biol Phys 2007;67:497–504.
[58] Weber DC, Rutz HP, Bolsi A, et al. Spot Scanning Proton Therapy in the Curative Treatment of Adult Patients with Sarcoma: the Paul Scherrer Institute Experience. Int J Radiat Oncol Biol Phys 2007.
[59] Weber DC, Rutz HP, Pedroni ES, et al. Results of spot-scanning proton radiation therapy for chordoma and chondrosarcoma of the skull base: the Paul Scherrer Institut experience. Int J Radiat Oncol Biol Phys 2005;63:401–9.
[60] Bues M, Newhauser WD, Titt U, Smith AR. Therapeutic step and shoot proton beam spot-scanning with a multi-leaf collimator: a Monte Carlo study. Radiat Prot Dosimetry 2005;115:164–9.
[61] Paganetti H, Bortfeld T. Proton therapy. In: Schlegel W, Bortfeld T, Grosu A-L, editors. New technologies in radiation oncology. Berlin: Springer; 2006.
[62] Jones DTL, Schreuder AN, de Kock EA, et al. Proton therapy at iThemba LABS. Radiat Phys Chem 2004;71:983–4.
[63] Meier MM, Amian WB, Goulding CA, Morgan GL, Moss CE. Neutron yields from stopping-length targets for 256 MeV protons. Nucl Sci Eng 1992;110:299–301.
[64] Maurer RH, Kinnison JD, Roth DR. Neutron production from 200–500 MeV proton interaction with spacecraft materials. Radiat Prot Dosimetry 2005;116:125–30.